Cell. Mol. Life Sci. (2013) 70:2585–2601
DOI 10.1007/s00018-013-1273-9

Cellular and Molecular Life Sciences

RESEARCH ARTICLE

Age-dependent changes in hippocampal synaptic transmission and plasticity in the $PLB1_{Triple}$ Alzheimer mouse

David J. Koss · Benjamin D. Drever · Sandra Stoppelkamp · Gernot Riedel · Bettina Platt

Received: 15 September 2012 / Revised: 14 January 2013 / Accepted: 21 January 2013 / Published online: 14 February 2013

Abstract Several genetically engineered models exist that mimic aspects of the pathological and cognitive hallmarks of Alzheimer's disease (AD). Here we report on a novel mouse model generated by targeted knock-in of transgenes containing mutated human amyloid precursor protein (APP) and microtubule-associated protein tau genes, inserted into the HPRT locus and controlled by the CaMKIIα regulatory element. These mice were crossed with an asymptomatic $presenilin1_{A246E}$ overexpressing line to generate $PLB1_{Triple}$ mice. Gene expression analysis and in situ hybridization confirmed stable, forebrain-specific, and gene-dose-dependent transgene expression. Brain tissue harvested from homozygous, heterozygous, and wild-type cohorts aged between 3 and 24 months was analyzed immunohistochemically and electrophysiologically. Homozygous $PLB1_{Triple}$ offspring presented with mostly intracellular cortical and hippocampal human APP/amyloid, first detected reliably at 6 months. Human tau was already uncovered at 3 months (phospho-tau at 6 months) and labeling intensifying progressively with age. Gene-dose dependence was confirmed in age-matched heterozygous females that accumulated less tau and amyloid protein. General excitability of hippocampal neurones was not altered in slices from $PLB1_{Triple}$ mice up to 12 months, but 2-year-old homozygous $PLB1_{Triple}$ mice had smaller synaptically evoked postsynaptic potentials compared with wild types. Synaptic plasticity (paired-pulse depression/facilitation and long-term potentiation) of synaptic CA1 pyramidal cell responses was deficient from 6 months of age. Long-term depression was not affected at any age or in any genotype. Therefore, despite comparatively subtle gene expression and protein build-up, $PLB1_{Triple}$ mice develop age-dependent progressive phenotypes, suggesting that aggressive protein accumulation is not necessary to reconstruct endophenotypes of AD.

Keywords Transgenic mice · Amyloid · Tau · Immunohistochemistry · Synaptic plasticity · LTP · LTD

D. J. Koss · B. D. Drever · S. Stoppelkamp · G. Riedel (✉) · B. Platt (✉)
School of Medical Sciences College of Life Sciences and Medicine, Institute of Medical Sciences, University of Aberdeen, Foresterhill, Aberdeen B25 2ZD, Scotland, UK
e-mail: g.riedel@abdn.ac.uk

B. Platt
e-mail: b.platt@abdn.ac.uk

Introduction

Alzheimer's disease (AD) is the most common form of dementia and is characterized by neurodegeneration in vulnerable forebrain regions such as the hippocampus, coupled with progressive memory loss and cognitive decline. Post-mortem, the disorder is identified by two pathological hallmarks defined as (1) extracellular amyloid plaques comprising an aggregation of the amyloid beta protein (Aβ) produced via the sequential cleavage of the amyloid precursor protein (APP) by secretase enzymes, and (2) intracellular neurofibrillary tangles composed of hyperphosphorylated forms of the microtubule-associated protein tau [1]. The cognitive symptoms of the disorder do not correlate particularly well with either plaque or tangle load; instead they correspond significantly with neuronal dysfunction, synaptic loss, and neurodegeneration [2]. More recently, a strong case has been made for the crucial role of soluble (especially oligomeric) amyloid species, and even intracellular levels of APP metabolites other than Aβ may be key contributors to neuronal malfunction [3–5].

Alterations in synaptic plasticity, the physiological parallel of learning, and memory, are key aspects of failing

neuronal function in dementia; hippocampal long-term potentiation (LTP) in particular is a recognized experimental indicator of cellular impairments observed in many models of the disorder [4, 6]. The sensitive nature of synaptic function, preceding detectable histopathological changes, has been repeatedly emphasized [7, 8], and is also often observed in non-transgenic AD models [9].

While the vast majority of AD cases (~95 %) are believed to be sporadic, i.e., there is no clearly identifiable underlying genetic cause, a small proportion of cases are familial in origin, termed familial AD (FAD), and result from mutations in the APP gene and presenilin 1 (PS1) gene, which forms the catalytic core of γ-secretase. The identification of such mutations coupled with the discovery of inherited mutations in the tau gene, responsible for tangle formation in certain frontotemporal tauopathies, has allowed the creation of numerous transgenic mouse models of AD, including Tg2576, PDAPP, and 3xTg-AD, which recreate various histopathological and cognitive aspects of the disease (e.g., [10]). However, their generation via pronuclear injection can result in random integration, unpredictable copy numbers, and unstable gene expression; and many models fail to create the entire spectrum of AD symptoms and the precise spatial and temporal pattern of disease progression [11, 12]. These factors contribute to the somewhat unreliable phenotype of such models and may explain the poor transition of treatments that showed promise in mouse models to clinical studies [13]. For these reasons, we recently created a new triple transgenic mouse model of AD, PLB1, through single-copy knock-in of mutated human versions of APP (Swe & Lon) and tau (P301L & R406W) into the HPRT locus and subsequent back-cross with a PS1 (A246E) line [14]. Initial characterization of these mice uncovered age-related, disease-relevant pathologies including human APP/Aβ, as well as tau and phosphotau proteins in the soma and processes of cortical and hippocampal neurones, in addition to sparse extracellular Aβ plaques; cognitive deficits in behavioral paradigms (see also [15]); sleep/wake changes alongside alterations in EEG spectral power; alterations in brain glucose metabolism; and deficits in hippocampal plasticity [14, 16].

Here, we set out to perform a more detailed transcriptional and translational tissue analysis and characterize hippocampal synaptic transmission and plasticity in $PLB1_{Triple}$ mice over the complete age spectrum (3–24 months), and compare mice with differing transgene load.

Materials and methods

Animals

The generation and genotyping of PLB1 mice has been described previously [14]. Briefly, these mice were created by the knock-in of a human APP-tau cDNA construct (hAPP: isoform 770 containing Swedish and London mutations; htau: isoform 4R with P301L and R406W mutations) into the HPRT locus and under the control of the mouse CaMKIIα promoter. $PLB1_{Double}$ mice were subsequently crossed with a homozygous presenilin 1 line ($PS1_{A246E}$ derived from an APP/PS1 line purchased from Jackson Laboratories [17], originally crossed with C57BL6 mice to remove the retinal *rd* mutation inherent to the C3H background) to produce triple transgenic (tg) animals. Due to the positioning of the HPRT locus on the X-chromosome, male transgenic mice were hemizygous (+) whereas females were either hetero- (+/−) or homozygous (+/+) for the transgenes.

$PLB1_{Triple}$ mice appeared of normal health and growth did not vary overall between transgenic genotypes and wild-type ($PLB1_{WT}$, "WT") littermates. All animals were maintained in acclimatized rooms (temperature: 22 °C; 12-h day/night cycle) with food and water ad libitum and procedures were carried out with institutional permission and according to the rules and regulations set out by the Home Office Animals (Scientific Procedures) Act, 1986.

Histologically, tissue was harvested from homozygous female $PLB1_{Triple+/+}$ mice ($n = 4$–6 per genotype and age group) aged between 3 and 21 months. Twenty-one-month-old WT and 12 to 13-month-old heterozygous $PLB1_{Triple+/-}$ were also stained.

For in vitro electrophysiology, the following mice aged 6 and 12 months were utilized: wild-type (WT; mixed gender, $n = 23$ at 6 months, $n = 16$ at 12 months), PS1 (A246E) homozygous (mixed gender, $n = 10$ at both 6 and 12 months) and $PLB1_{Triple}$ (APP/tau/PS1) heterozygous ($PLB1_{Triple+/-}$; female, $n = 15$ at 6 months; $n = 11$ at 12 months), homozygous ($PLB1_{Triple+/+}$; female, $n = 11$ at 6 months, $n = 16$ at 12 months) and hemizygous ($PLB1_{Triple+}$; male, $n = 13$ at 6 months, $n = 11$ at 12 months). Additionally, slices from $PLB1_{Triple+/+}$ and WT mice were characterized at 3 and 24 months of age (WT: $n = 12$ at 3 months, $n = 11$ at 24 months, $PLB1_{Triple+/+}$: $n = 10$ at 3 months; $n = 9$ at 24 months).

Molecular biology and histology

RNA extraction and quantitative real-time PCR

Forebrain samples (4 mm^3) were dissected from $PLB1_{Triple}$ and age-matched wild-type mice and immediately stored in RNA Later solution (Qiagen Sussex, UK) at 4 °C over night, then at −20 °C until extraction. Total RNA was extracted with RNeasy Lipid Tissue Mini Kit (Qiagen, Sussex, UK) according to the manufacturer's instructions, including homogenization via Qiashredder and on-column DNaseI (Qiagen, Sussex, UK) digests to minimize genomic DNA contamination. Only integrity-controlled RNA (Bioanlayser,

performed by the Rowett Institute, Aberdeen) with a RIN score above 7 was used for expression analyses. cDNA synthesis was performed in 20-µl reactions containing 2 µg total RNA, 60 µM random hexamer primers, 8 mM $MgCl_2$, dNTPs 1 mM each, 20 U RNase inhibitor, 5 mM DTT, and 10 U Transcriptor High Fidelity Reverse transcriptase (Roche, Burgess Hill, UK) in 50 mM Tris/HCl, 30 mM KCl for 30 min at 50 °C, 5 min 85 °C. The obtained cDNA was then diluted 1:5 with RNase free water and frozen at −20 °C until needed. Gene expression analysis was carried out with the Bio Rad MiniOpticon Real-Time PCR Detection System using iQ SYBR Green Supermix (Bio-Rad, Hemel Hempstead, UK) in a final volume of 20 µl. 100 ng cDNA equivalent were run in triplicates per sample with 3.2 µM each gene specific oligomer primers: human APP: 5′-ACT GGC TGA AGA AAG TGA CAA-3′ (forward) and 5′-ATC ACC ATC CTC ATC GTC CTC G-3′ (reverse); human tau: 5′-CAC GGA CGC TGG CCT GAA AG-3′ (forward) and 5′-CTG TGG TTC CTT CTG GGA TC-3′ (reverse). Housekeeping gene mouse GAPDH primers 5′-ACT TTG TCA AGC TCA TTT CC-3′ (forward) and 5′-TGC AGC GAA CTT TAT TGA TC-3′ (reverse) were generously provided by Dr Alun Hughes, University of Aberdeen. The thermocycler profile consisted of 3 min at 95 °C initial denaturation followed by 36 cycles of 30 s at 95 °C, 20 s at annealing temperature (hAPP 65 °C, htau 63 °C, mGAPDH 60 °C) when the fluorescence was monitored. Negative cDNA reactions (excluding reverse transcriptase) and no template controls ensured that no contamination by genomic DNA altered the results. Quantification was obtained by comparing the fluorescence intensities against standard serial dilutions of plasmids containing 20 to 2×10^5 copies of the human transgenes, or 2×10^3–2×10^7 copies of the mouse housekeeping gene. Melting curve analyses ensured specific amplification products of the samples. Data analyses were performed using Opticon Monitor Software (Bio-Rad, Hemel Hempstead, UK). Absolute gene expression (copy number) of each sample was normalized to the arithmetic mean of the endogenous controls. Experimental data are expressed as arithmetic means +SEM. Statistical analyses were performed with GraphPad Prism software (version 5.01, GraphPad Software Inc., San Diego, USA) using one-way ANOVA test to establish significant differences followed by individual *t* tests of selected data pairs. $p < 0.05$ was considered significant.

Tissues harvesting and histology

Mice were terminally anaesthetized and tissue fixed in situ by intra-aortic perfusions of 4 % paraformaldehyde in 0.1 M phosphate buffer. Brains were removed, post-fixed for 4 h, and subsequently transferred into 1.4 % Na Cacodylate storage buffer (w/v) and subsequently wax embedded and sectioned. This procedure was modified from our previous publication [14], to enhance intracellular epitope detection, as we here found that fixation conducted for ~24 h prior to embedding affected intracellular amyloid detection while staining of plaques was sustained.

Slide-mounted coronal sections (5 µm) were used for DAB-based immunochemical staining conducted with the Leica/bond autostainer (Leica Microsystems, Milton Keynes, UK). Sections underwent automated dewaxing, acidic antigen retrieval and appropriate antibody application. Immuno-labeling was conducted using 6E10 for human APP/Aβ (1:200, Cambridge Bioscience, UK), HT-7 for human tau (1:200, Autogen-Bioclear, Wiltshire, UK), and AT-8 (1:25, Autogen-Bioclear) and PS-396 (1:200, Santa Cruz) for phospho-tau. Primary antibodies were visualized using Bonds refined DAB staining kit (Leica Microsystems); nuclei were counterstained using hematoxylin.

All images were taken via a digital camera (Axocam) connected to a Zeiss microscope (Axioskop 2 plus) with a water immersion lens (10× or 40×), using Axiovision software (Zeiss, Hertfordshire, UK).

In situ hybridization

Coronal sections (15 µm) were prepared from frozen brain samples fixed for 5 min in ice cold buffered 4 % Paraformaldehyde solution, washed in cold PBS, submerged in 70 % ethanol for 5 min and finally stored in 95 % ethanol at 8 °C until processing. For in situ hybridization, slides were dried and incubated with ^{35}S terminal transferase-labeled oligonucleotides (hAPP: 5′-CAG ATT CAC TTC AGA GAT CTC CTC CGT CTT GAT ATT TGT CAA CCC AGA AC-3′; htau: 5′-CTC AGG TCA ACT GGT TTG TAG ACT ATT TGC ACA CTG CCG CCT CCC GAG AC-3′) over night at 42 °C. After washing off unbound probes, the sections were exposed to autoradiograph film for 6 weeks. The specificity of the labeling was assessed by co-incubation of brain sections with 100-fold excess of unlabeled towards labeled oligonucleotide.

In vitro electrophysiology

Slice preparation and recording conditions were conducted as described previously [14, 18]. Briefly, animals were injected intraperitoneally with a lethal dose of euthatal and killed by decapitation when unconscious. The brains were quickly removed into ice-cold sucrose-based artificial cerebrospinal fluid (aCSF; composition in mM): 249.2 sucrose, 1.5 KCl, 1.3 $MgSO_4$, 0.96 $CaCl_2$, 1.5 KH_2PO_4, 2.89 $MgCl_2 \cdot 6H_2O$, 25 $NaHCO_3$ and 10 glucose (pH 7.4, continuously gassed with 95 % O_2/5 % CO_2), and the hippocampus dissected. Hippocampal slices (400 µm) were prepared with a McIllwain tissue chopper and stored in oxygenated

standard aCSF (composition as above except sucrose replaced with 129.5 mM NaCl and concentration of $CaCl_2$ increased to 2.5 mM) at 32 °C for at least 1 h before experiments commenced.

Recordings of CA1 field excitatory postsynaptic potentials (fEPSPs) were undertaken in an interface chamber perfused at a rate of approximately 5 ml min^{-1} with pre-warmed, gassed aCSF, and recorded via an aCSF-filled borosilicate glass electrode (3–7 MΩ) positioned in the *stratum radiatum* after stimulation of the Schaffer collateral/commissural fibres by a monopolar stimulation electrode (WPI, UK, 0.5 MΩ). The signal passed through the recording electrode to a CV203BU headstage pre-amplifier with a gain of 1 (Axon Instruments, CA, USA) connected to an Axoclamp 200B amplifier (Axon Instruments). A CED 1401 Plus (Cambridge Electronic Design Ltd., Cambridge, UK) digitized the analogue signal for passage to a PC, where data was acquired using the P-WIN software package (Leibniz Institute for Neurobiology, Magdeburg, Germany).

By increasing the stimulus intensity in a stepwise manner until saturation was reached, input/output (IO) curves of basic synaptic transmission were generated. For all groups, a stimulus intensity of 40–50 % of saturation was applied to run subsequent LTP experiments. Baseline responses were recorded for at least 10 min (responses recorded every 30 s, response variability <10 %) and LTP evoked by applying a theta burst tetanus [5 Hz, five bursts of four stimuli (100 Hz), inter-burst interval of 200 ms for 1 s]. Recording continued for 60 min post-tetanus. Long-term depression (LTD) experiments followed a similar time course, with the theta burst tetanus replaced with 900 pulses at 1 Hz, which induced a long-lasting depression of synaptic responses. Further, a paired-pulse protocol investigated changes in presynaptic release mechanisms and short-term plasticity. Pairs of identical stimuli (inter-stimulus interval (ISI): 10, 40, 100, and 200 ms) were delivered at a stimulus intensity 60 % of that which caused saturation in IOs.

Data analysis

Data were averaged and are presented as group means (+SEM) with all statistical analysis performed using GraphPad Prism software (V5; GraphPad Software, San Diego, CA, USA). IO curves of fEPSP slope vs. stimulus intensity were generated and compared between groups via a two-way ANOVA (genotype × stimulus). Comparison between groups applied non-linear regression analysis, and determined mean IO curves, maximum fEPSP slopes, stimulus intensity required to illicit 50 % of the maximum response and Hill slopes (extra sum of squares *F* test). For IO curves of fEPSP slope vs. fiber volley amplitude, only signals that allowed reliable measurement of the presynaptic volley were included. Each IO was subject to curve-fitting (sigmoidal dose–response variable slope paradigm) and from the resulting curves fEPSP slopes for fiber volleys of 0–0.5 mV were calculated. The data for each group was then collated and analyzed as above.

LTP and LTD time courses of fEPSP slopes were calculated relative to baseline values (=100 %) and evaluated using repeated-measures (RM) ANOVA to compare post-tetanus values between groups (genotype × time). Paired pulse responses were calculated as the ratio of the second response relative to the first (S2/S1 in %), with overall group analysis carried out via a two-way ANOVA (genotype × ISI) and post hoc Student's *t* tests to compare individual ISIs. Significance was assumed for $p < 0.05$.

Results

$PLB1_{Triple}$ mice have stable gene expression

Due to the targeted knock-in as opposed to random integration of transgenes, $PLB1_{Triple}$ mice were expected to have stable and consistent gene expression. This was confirmed by quantitative real-time PCR, determining copy numbers of transgenes normalized to copy numbers of the endogenous mouse GAPDH. No hAPP or htau mRNA was present in WT mice ascertaining the specificity of primers for human transgenes, while the tenfold lower expression levels in the cerebellum compared with the forebrain corroborated the regional specificity of the CaMKIIα promoter (Fig. 1a). This regional distribution was additionally confirmed by in situ hybridization with a signal strongest in the hippocampus (Fig. 1c). Differences in mRNA expression levels between $PLB1_{Triple+/-}$, $PLB1_{Triple+}$, and $PLB1_{Triple+/+}$ animals investigated any influence of the X-chromosomal insertion site. As expected with random inactivation of one X-chromosome, $PLB1_{Triple+/-}$ mice had about half the levels of transgenic mRNA expression (hAPP or htau, respectively) compared with $PLB1_{Triple+}$ or $PLB1_{Triple+/+}$, which were not different from each other (Fig. 1a). Due to this similarity in mRNA expression, data from $PLB1_{Triple+}$ and $PLB1_{Triple+/+}$ animals were subsequently pooled (Fig. 1b). In older WT and transgenic animals, expression of the GAPDH housekeeping gene was unaltered; the relative expression levels were determined without further adjustments. Postnatal GAPDH mRNA expression, however, was lower compared with older animals but still unaltered between WT and transgenic animals (data not shown). To compare mRNA expression between age groups, GAPDH expression levels were adjusted to the postnatal stage (0 day) prior to normalization of human transgenes. Intriguingly, htau mRNA expression was similar at postnatal day 0 and at 6 and 12 months of age; hAPP expression was lower at birth (day 0) but stable at 6 and

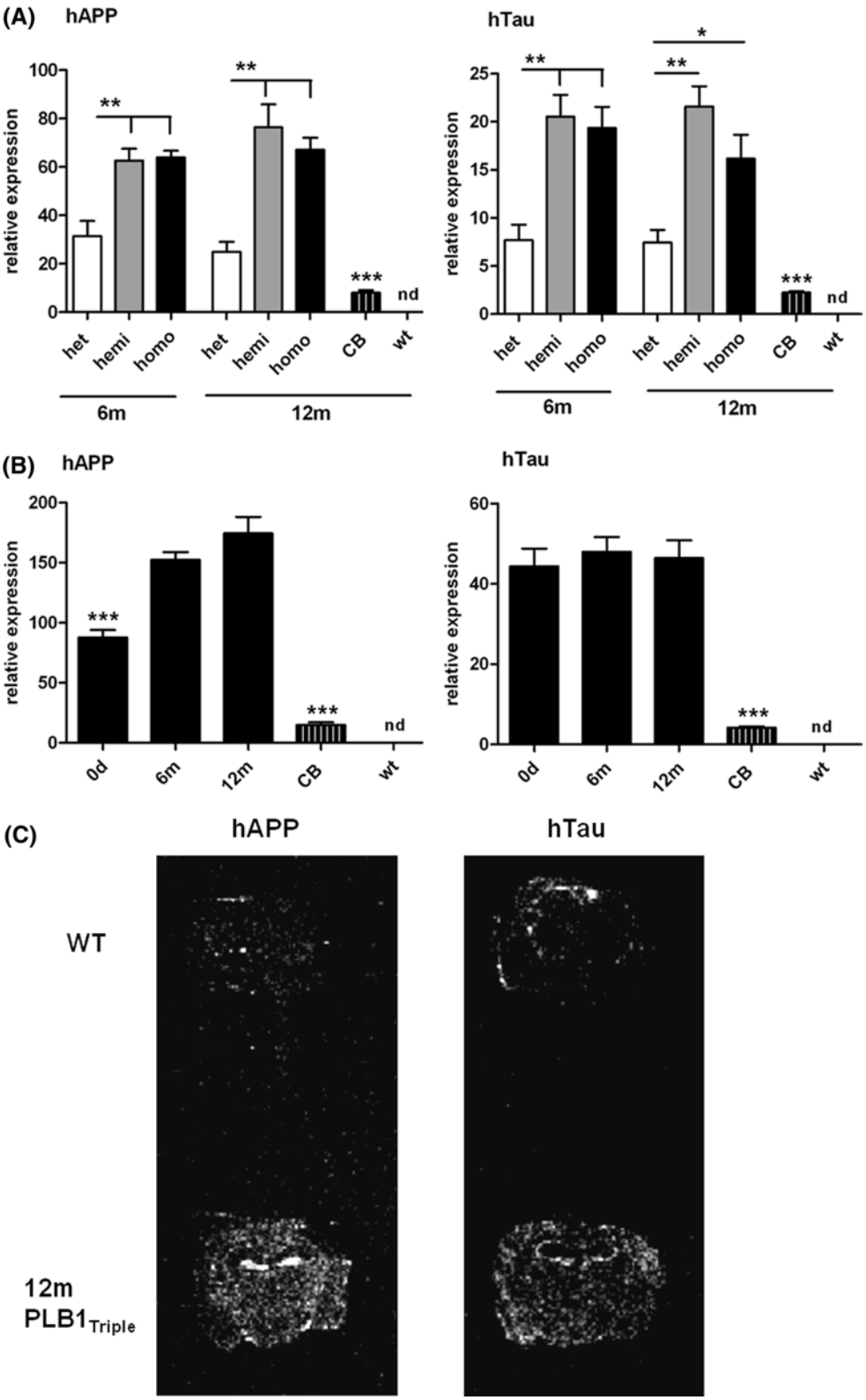

Fig. 1 mRNA expression of human APP and tau transgenes is stable in adult $PLB1_{Triple}$. **a** Human APP and tau mRNA expression was not significantly different between $PLB1_{Triple+}$ ("hemi"; 6 months $n = 5$; 12 months $n = 4$) and $PLB1_{Triple+/+}$ ("homo"; 6 months $n = 5$; 12 months $n = 3$) mice, while mRNA expression in $PLB1_{Triple+/-}$ animals ("het"; 6 months $n = 5$; 12 months $n = 4$) was twofold lower. No transgenic product was detected in wild-type (wt) animals ($n = 8$) and expression levels in the cerebellum (CB, $n = 7$) were negligible, i.e., >tenfold lower than in forebrain samples. **b** Human tau mRNA expression was unaltered in neonates ($n = 11$) vs. adult animals (6 months $n = 10$; 12 months $n = 7$). mRNA expression levels of human APP were not significantly different in adult animals but significantly lower in neonates. General expression levels of human APP were about threefold higher than human tau expression. Shown are mRNA copy numbers normalized to mouse GAPDH expression (endogenous control) +SEM. An overall ANOVA followed by individual *t* tests confirmed significant differences (indicated above the *bars*) compared with 6- and 12-month data sets. $*p < 0.05$; $**p < 0.01$; $***p < 0.001$; *nd* not detected, *m* month. **c** In situ hybridization confirmed low but region-specific transgene expression in 12-month-old $PLB1_{Triple}$ animals for both hAPP and htau, and lack of expression in $PLB1_{WT}$ (WT)

12 months. This absolute quantification enabled direct comparison of transgene levels, which yielded threefold lower htau mRNA expression than hAPP and is most likely explained by faster 3′ degradation.

Age-dependent progression in pathology in $PLB1_{Triple}$ mice

Immunohistochemical analysis was performed in $PLB1_{Triple+/+}$ and $PLB1_{Triple+/-}$ specimens aged 3–21 months.

A largely pre-plaque stage of 3 months was revealed for both cortex and hippocampus (Fig. 2); with weak intracellular stain apparent. A notable increase in 6E10 immunoreactivity was consistently observed throughout the forebrain by 12 months of age. Immunoreactivity was most intense within the somata of pyramidal neurons in the hippocampus and cortex, but reactivity extended into the neuropil. Interestingly, processes of cortical neurones already displayed stained processes at 6 m, while such staining occurred only at 12 months in hippocampal neurones. Overall, an age-dependent strengthening of staining was visible, suggesting a progressive intracellular accumulation of 6E10 reactive substrates. Some faint APP/Aβ labeling was detected in aged (21 months old) WT brains, presumably due to a degree of cross reactivity of the 6E10 antibody with endogenous murine APP and its metabolites. Such staining is unavoidable as low transgene expression resulting from single copy knock-in requires the use of relatively high antibody concentrations. Nevertheless, specific and reproducible staining in sub-cellular compartments was only apparent in transgenic mice.

In parallel sections, tau protein was labeled by three antibodies: HT-7 as a specific human tau marker, and AT-8 and PS-396 to reveal phosphorylated tau. Specificity was again

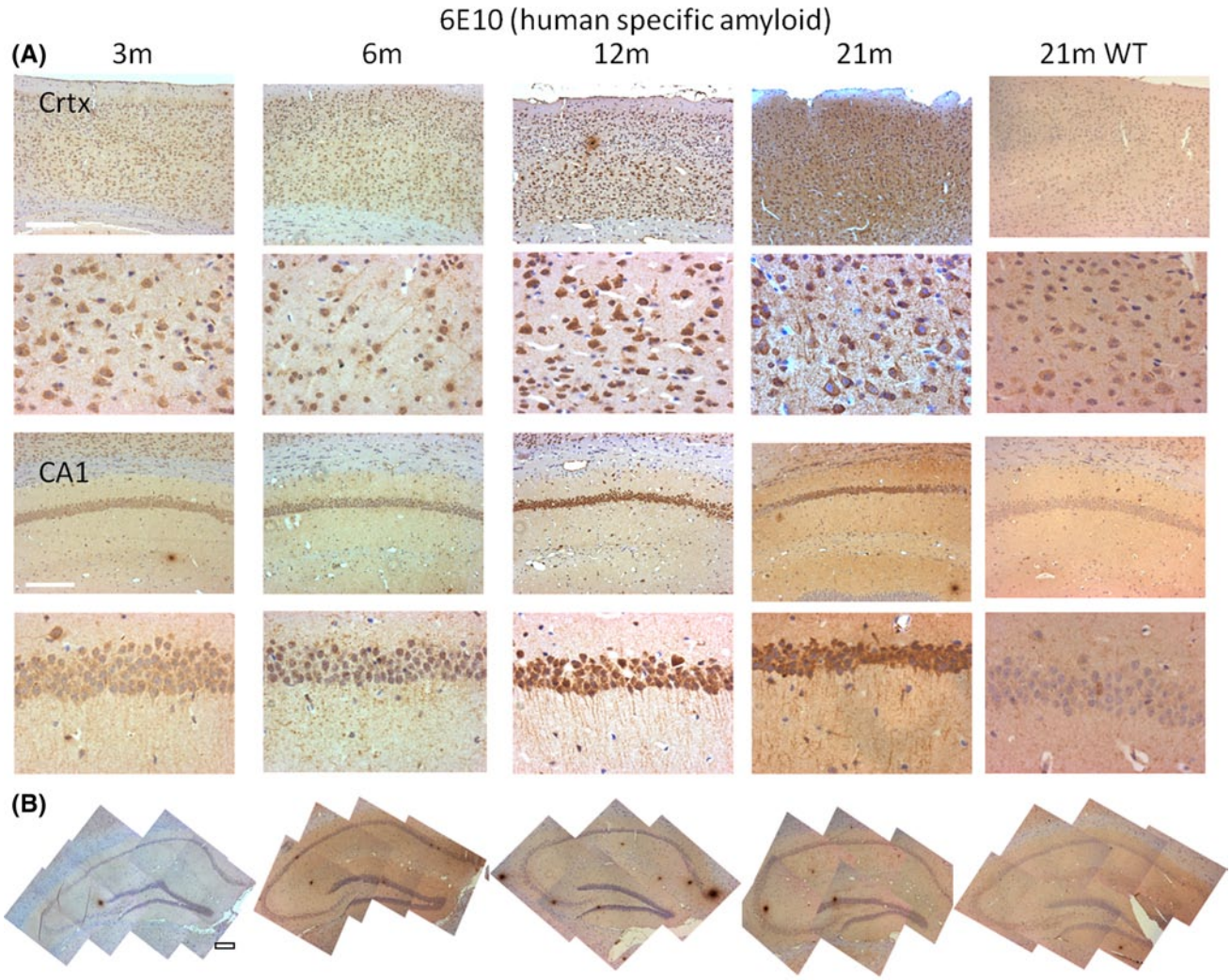

Fig. 2 Amyloid histopathology in $PLB1_{Triple}$ mice aged between 3 and 21 months. Coronal sections labeled with antibody 6E10 targeted toward amino acid sequence 1–16 of human Aβ, see "Methods" for details. **a** Only subtle somatic staining, matching that of aged (21 months) $PLB1_{WT}$ mice (WT), was observed in $PLB1_{Triple}$ mice at 3 months of age. Rare and defuse extracellular plaques were present from 6 months in both cortex (Crtx) and hippocampal CA1. Subtle intracellular staining primarily within the processes of neurones is also visible, but only reliably detected from 12 months onwards. Images were taken at ×10 and ×40 magnification; *scale bars* 200 μm. **b** Micrographs of hippocampal montages demonstrating age-dependent yet rare occurrence of plaques. Images taken at ×10 magnification, *scale bar* 200 μm

confirmed in 21 months WT brains which were devoid of HT-7 immunoreactivity (Fig. 3). Human tau expression was already present in forebrain principle cells at 3 months in $PLB1_{Triple}$ brains and intensified over time. At 12 months, dense labeling in somata and processes in cortex and CA1 was revealed, followed by a decline in somatic tau staining at 21 months amidst stronger tau immunoreactivity in CA1 neurites. Phosphorylated tau was detected in somatic and dendritic compartments from 6 months with both AT-8 and PS-396 antibodies (Fig. 4). Interestingly, both HT7 and hippocampal AT-8 staining was particularly intense at 12 months with extensive dendritic staining, while somatic PS-396 staining peaked at 21 months.

We also compared immunoreactivity between $PLB1_{Triple+/-}$ and $PLB1_{Triple+/+}$ at 12–13 months. In agreement with their gene expression profile, tau (Fig. 5a, HT-7) and APP/Aβ (Fig. 5b, 6E10) staining was weaker in heterozygous ("Hets") $PLB1_{Triple+/-}$ tissue in both cortex and CA1. In particular, APP/Aβ-positive staining was weakly detectable in cortex and hippocampus of $PLB1_{Triple+/-}$ brains and only small plaques were evident; intracellular staining was limited to a diffuse staining of the somata of pyramidal neurons with little reactivity in processes. Tau immunoreactivity in $PLB1_{Triple+/-}$ brains was detected in identical neuronal compartments as in $PLB1_{Triple+/+}$, it was, however, apparent that the number of labeled neurons as well as the overall intensity was much reduced in $PLB1_{Triple+/-}$ mice.

Alterations in hippocampal physiology in $PLB1_{Triple}$ mice appear at 6 months

Since $PS1_{A246E}$ mice were utilized to generate $PLB1_{Triple}$ mice, it was first necessary to characterize these electrophysiologically. Our previous study [14] only evaluated the

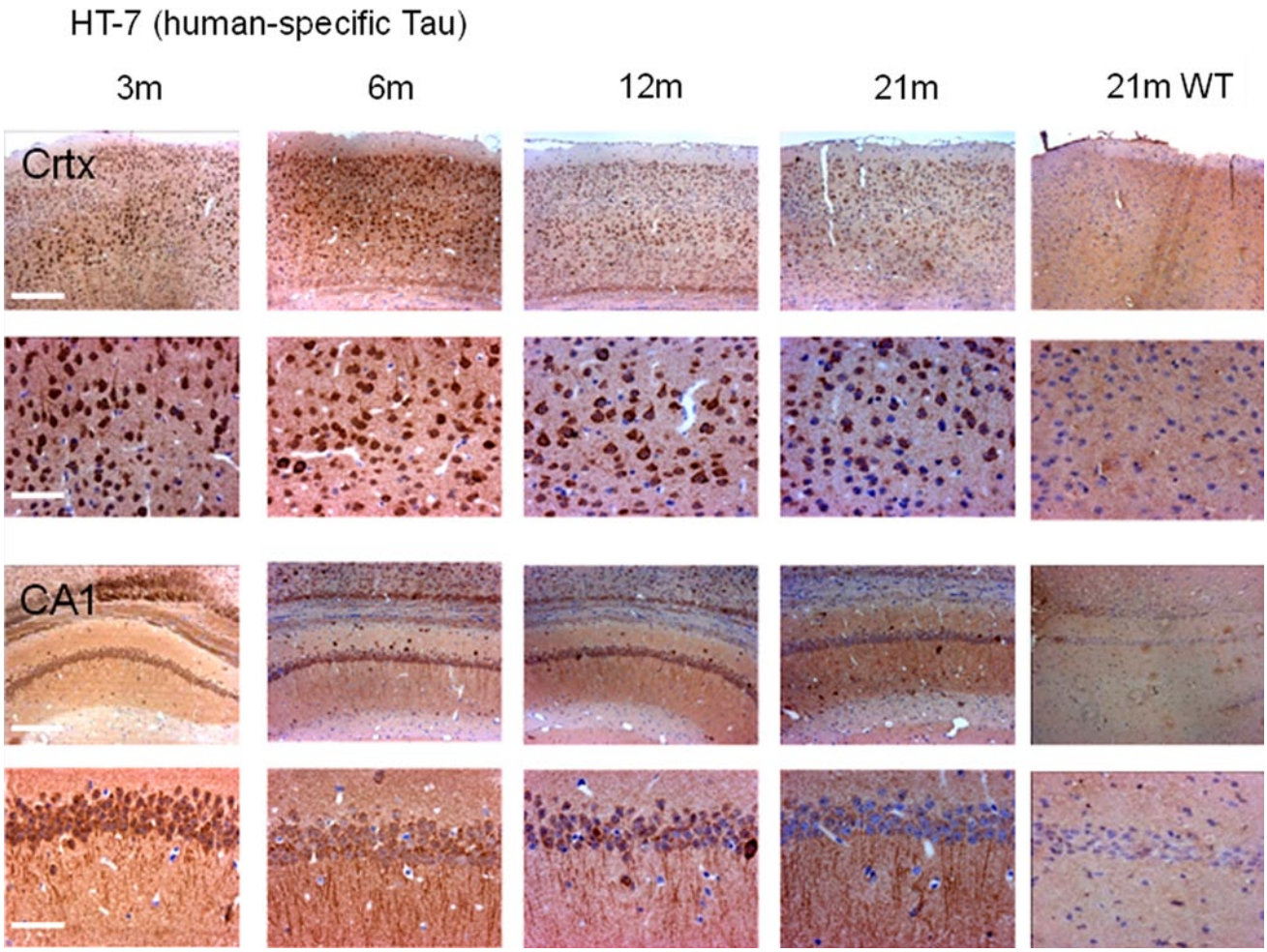

Fig. 3 Human tau expression in $PLB1_{Triple}$ mice is present at 3 months. Coronal sections labeled with HT-7 antibody targeted toward the human specific tau sequence (see "Methods" for details). Positive staining was seen in somata and neurites of principle cells in cortex (Crtx) and hippocampal CA1. Human tau accumulated from 3 months, with strongest HT-7 immunoreactivity present at 12 months. At 21 months, a subtle decrease of somatic intracellular staining was apparent. No positive staining was visible in WT. Images were taken at ×10 and ×40 magnification; *bars* indicate 200 and 50 μm, respectively

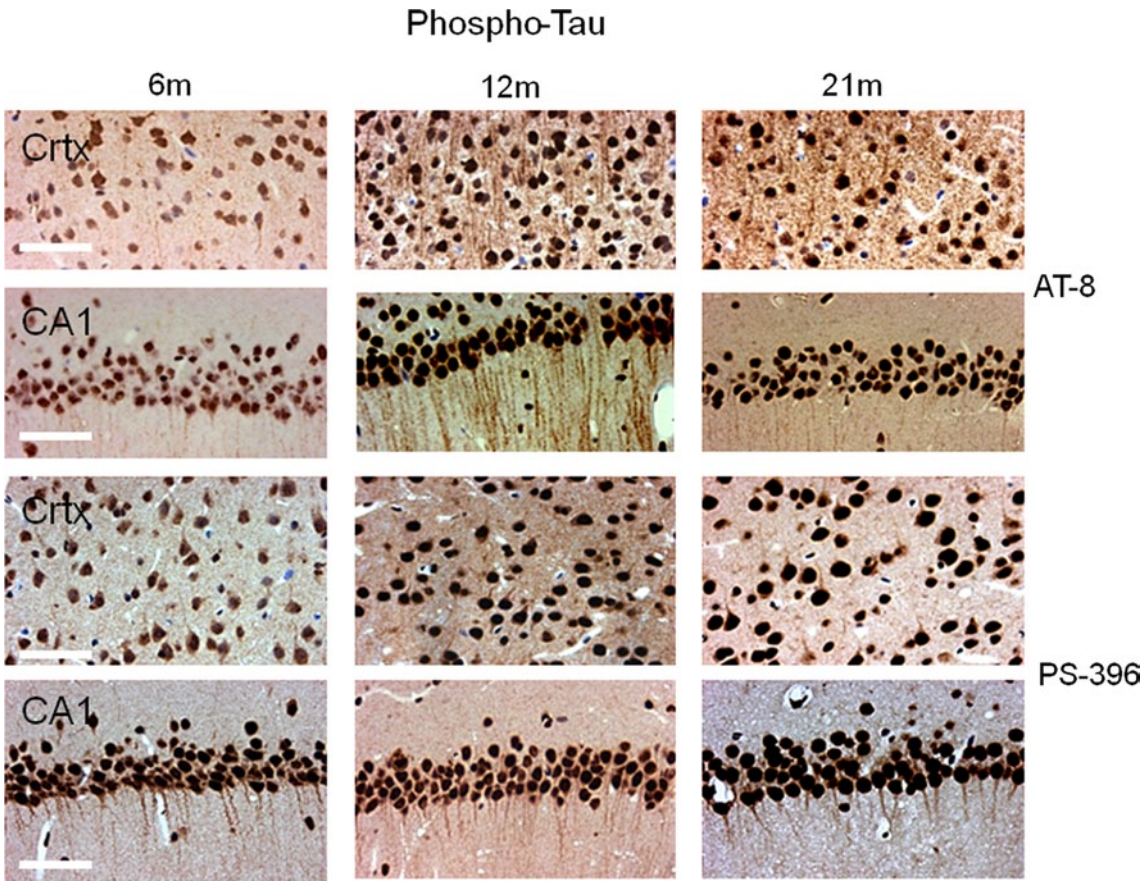

Fig. 4 Tau phosphorylation in $PLB1_{Triple}$ mice. Coronal sections labeled with phospho-tau antibodies AT-8 and PS-396. Positive staining was identified from 6 months of age in somata and processes of cortical neurons (Crtx) and hippocampal neurons (CA1). Similar to human tau expression (HT-7, see Fig. 3), an accumulation of phospho-tau was evident with robust immunoreactivity within cell bodies and processes of both cortical and CA1 neurons. Interestingly, while PS-396 staining intensified further at 21 months, AT-8 staining peaked at 12 months, indicative of a shift in tau processing with increasing age. Images taken at ×40 magnification, *scale bar* 50 μm

lack of PS1-related changes in paired pulse behavior; we now also confirm that no significant changes in any of the physiological parameters investigated were found in PS1 mice (all p values > 0.05), indicating intact CA3-CA1 synaptic responses and plasticity in these mice (Figs. 6, 7, 8).

Therefore, altered hippocampal physiology and plasticity in $PLB1_{Triple}$ animals can be attributed to the expression of hAPP and/or htau transgenes in combination with PS1. When slices from $PLB1_{Triple+/+}$ mice were compared with WT at 3 months of age, no significant alterations in IO relationships (plotted vs. fiber volley or stimulus intensity, Fig. 6a, b), paired pulse responses (Fig. 7a), LTP (Fig. 8a), or LTD (Fig. 9a) were evident, confirming this to be a baseline age with unaltered hippocampal physiology. We reasoned that the lack of any obvious phenotype in homozygous mice at this young age negated the need to investigate responses in $PLB1_{Triple+/-}$ or $PLB1_{Triple+}$ mice.

When plotting fEPSP slope against stimulus intensity, IO curves of 6- and 12-month-old groups investigated were also not significantly different to $PLB1_{WT}$ (Fig. 6e, g). Furthermore, non-linear regression analysis of the curves indicated no significant differences between groups in terms of maximum fEPSP slope, stimulus intensity required to elicit 50 % of maximum response and Hill slopes of the curves (p values > 0.05). As measuring fEPSP slopes vs. stimulus intensity only serves as an indicator of maximal post-synaptic responses and does not calibrate these responses relative to presynaptic activation, we also analyzed fEPSPs relative to the amplitude of the presynaptic fiber volley (Fig. 6 b, d, f, h). Under these conditions, findings at 6 months were confirmed; i.e., basic synaptic transmission was intact in all $PLB1_{Triple}$ mice (Fig. 6d). In contrast, significant deficits were detected at 12 months in the $PLB1_{Triple+}$ [F (1,248) = 4.1, p < 0.05] and $PLB1_{Triple+/+}$ groups [F (1,218) = 9.4, p < 0.01], but not in the $PLB1_{Triple+/-}$ group compared with WT (Fig. 6e). Thus, homozygous and hemizygous $PLB1_{Triple}$ mice presented with deficits in basic synaptic transmission at 12 months of age.

We next investigated how these parameters changed in $PLB1_{Triple+/+}$ mice at 24 months of age (Fig. 6g,h). Here,

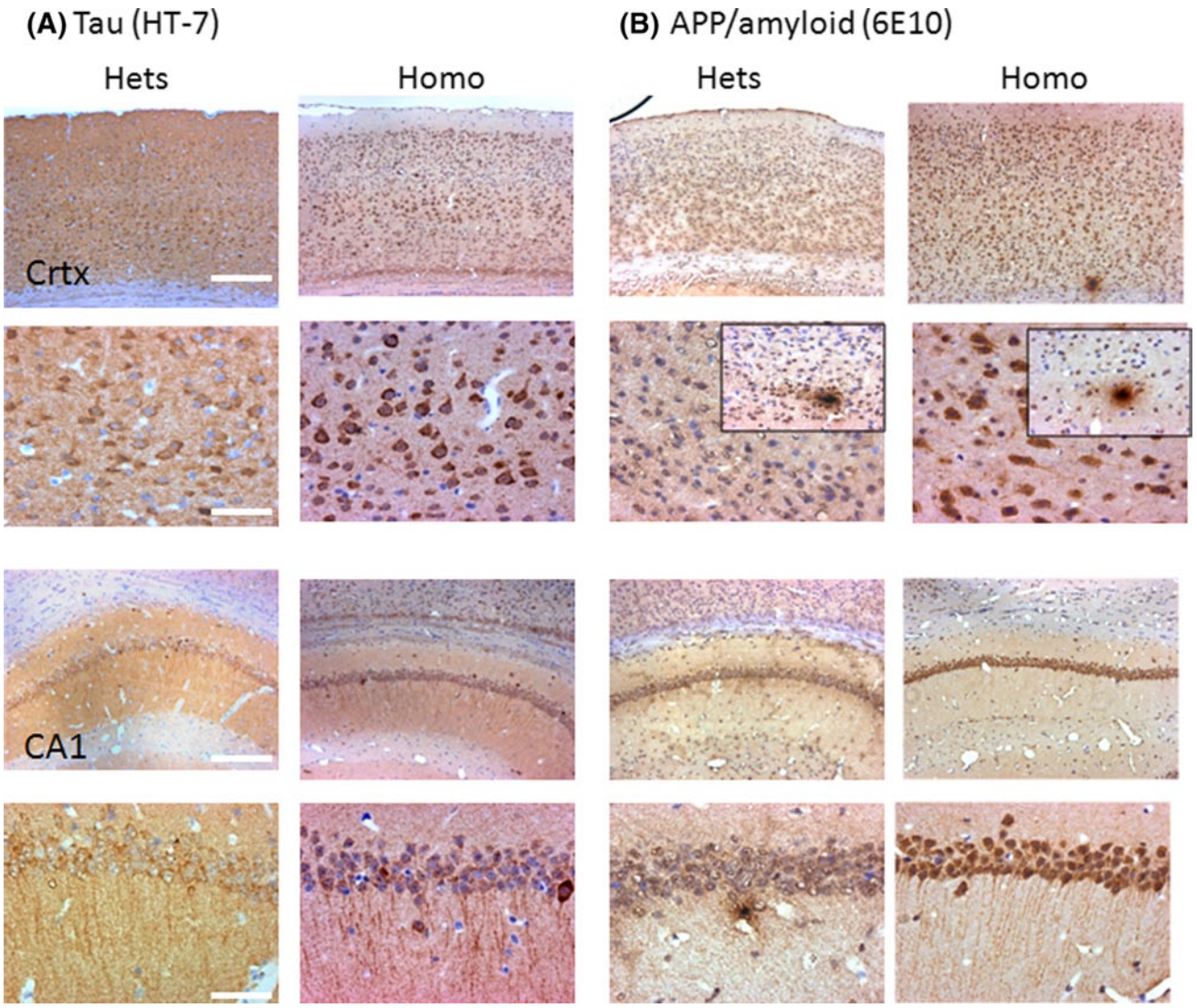

Fig. 5 Comparison of human tau and amyloid expression in $PLB1_{Triple+/-}$ and $PLB1_{Triple+/+}$ mice at ~12 months. **a** Coronal sections labeled for tau with HT-7 confirmed stronger immunoreactivity in homozygous ("Homo") compared to heterozygous ("Hets") specimen particularly in cortex (Crtx); somata and neuropil were stained in both genotypes. **b** Intracellular APP/amyloid staining via 6E10 in $PLB1_{Triple+/-}$ was weak in cortex and more diffuse in CA1 compared to $PLB1_{Triple+/+}$ mice, only the latter showed distinct axonal staining. Rare cortical plaques in $PLB1_{Triple+/-}$ appeared small and more diffuse (see *Insert*). Images taken at ×10 and ×40 magnification; *scale bars* represent 200 μm

severe deficits in basic synaptic transmission were evident in transgenic mice both in fEPSP slope vs. stimulus intensity and fEPSP slope vs. fiber volley IO curves (genotype effect: both p values < 0.0001). In the fEPSP slope vs. stimulus intensity IO, this deficit manifested itself as a reduction in the maximum response (extra sum-of-squares F test $p = 0.0004$), as the Hill slope and stimulus intensity required to elicit 50 % of maximum response were not significantly different. The responses were also significantly different to those at 12 months, indicating a deterioration in synaptic transmission between these time points (age effect: both p values <0.0001).

Synaptic plasticity is impaired in $PLB1_{Triple}$ mice from 6 months of age

Paired pulse stimulation

A paired pulse paradigm was employed to investigate alterations in presynaptic transmitter release and putative changes in short-term plasticity. In all genotypes, an ISI of 10 ms induced paired pulse inhibition (PPI), while ISIs of 40, 100, and 200 ms induced varying degrees of paired pulse facilitation (PPF; Fig. 7). No difference in PPI or PPF was observed between $PLB1_{WT}$ and $PLB1_{Triple+/+}$ mice aged 3 months

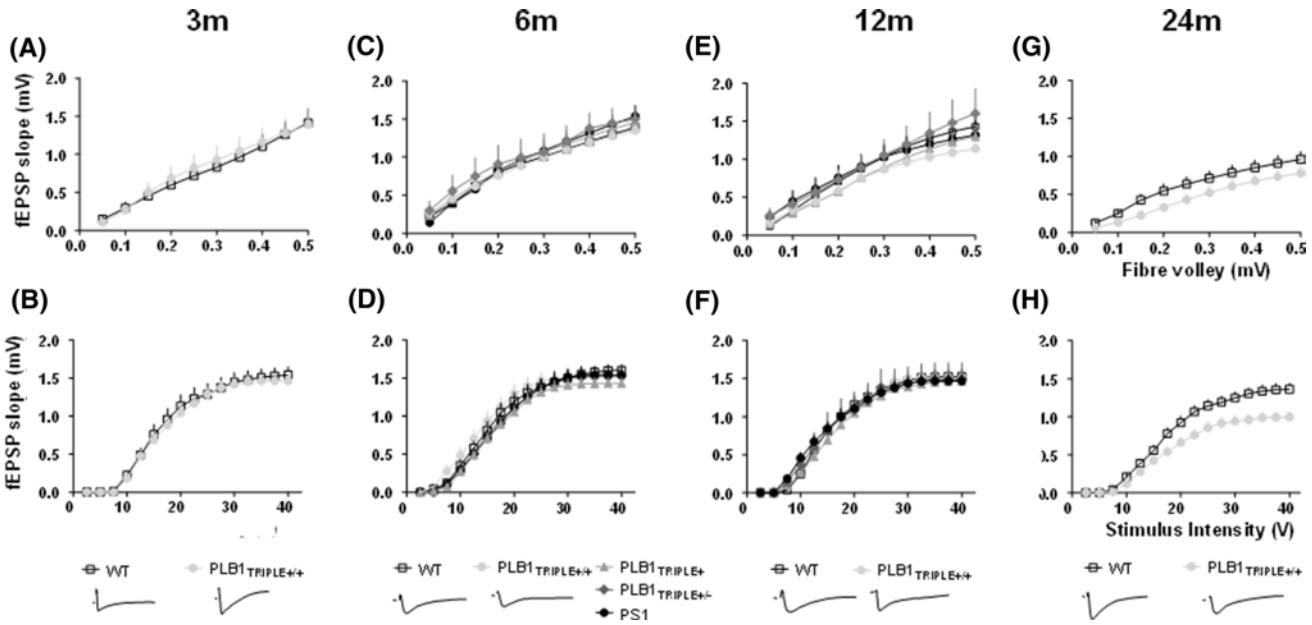

Fig. 6 Basic synaptic transmission is reduced in $PLB1_{Triple}$ mice from 12 months onwards. IO curves of basic synaptic transmission are shown with fEPSP slope (means + SEM) plotted against stimulus intensity and presynaptic fiber volley amplitude. (A, B) No changes were apparent in $PLB1_{Triple+/+}$ ($n = 24$) mice at 3 months compared with WT ($n = 26$). (C, D) At 6 months, basic synaptic transmission was intact in $PLB1_{Triple+/+}$ ($n = 12$), $PLB1_{Triple+}$ ($n = 13$), $PLB1_{Triple+/-}$ ($n = 19$) and PS1 ($n = 18$) mice versus WT ($n = 16$). (E, F) Synaptic transmission was impaired in $PLB1_{Triple+/+}$ ($n = 18$, $^{**}p < 0.01$) and $PLB1_{Triple+}$ ($n = 12$, $^{*}p < 0.05$) mice at 12 months but intact in $PLB1_{Triple+/-}$ ($n = 11$) and PS1 ($n = 18$) mice relative to WT ($n = 26$), for data plotted against fiber volley amplitude. (G, H) At 24 months, there was a further reduction in evoked responses in the $PLB1_{Triple+/+}$ group ($n = 31$, $^{***}p < 0.0001$) in relation to WT ($n = 40$). Sample traces for selected groups are also illustrated

(Fig. 7a). As this group presented with the highest level of pathology, we did not examine hetero or hemizygous mice in this age range.

Significant deficits in PPF were found in $PLB1_{Triple+/-}$, $PLB1_{Triple+}$ and $PLB1_{Triple+/+}$ groups at 6 months (Fig. 7b). Overall analysis of paired pulse responses revealed significant effects with factor genotype in all transgenic groups tested (F values > 3; p values < 0.05). Effects were somewhat dependent on transgene load ($PLB1_{Triple+/-}$: p values < 0.05; $PLB1_{Triple+/+}$: p values < 0.01; $PLB1_{Triple+}$: p values < 0.0001), post hoc analysis confirmed significant deficits in PPF for ISIs of 100 ms in the $PLB1_{Triple+/-}$ group, 100 and 200 ms in the $PLB1_{Triple+}$ group, and 40, 100, and 200 ms in the $PLB1_{Triple+/+}$ group (see asterisks in Fig. 7b).

There were similar findings at age 12 months (Fig. 7c). Significant deficits in PPF were found in all 12-month triple transgenic groups compared with WT. Overall analysis of the responses indicated a significant main effect of genotype for all transgenic groups, again progressively increasing with transgene expression $PLB1_{Triple+/-}$ [F (1,100) = 4.8, $p < 0.05$], $PLB1_{Triple+}$ [F (1,100) = 5.2, $p < 0.05$] and $PLB1_{Triple+/+}$ groups [F (1,100) = 6.0, $p < 0.05$] versus WT. As indicated by asterisks in Fig. 7c, further examination of fEPSP slope data yielded significant PPF deficits in $PLB1_{Triple+/-}$ and $PLB1_{Triple+}$ groups for an ISI of 40 and in all three triple transgenic mouse lines for an ISI of 100 ms. Note that no phenotype was revealed for homozygous PS1 animals at either 6 or 12 months.

Although paired pulse responses were not significantly different in $PLB1_{Triple+/+}$ mice at 24 months compared with WT, there was a strong trend for a significant deficit [F (1,95) = 3.3, $p = 0.07$] and post hoc t test analysis confirmed reduced PPF in the transgenic group for an ISI of 40 ms (Fig. 7d asterisk). The likely reason for the reduced severity in the deficits in short-term plasticity at this age is due to reduced PPF in the WT group at this age compared with younger time points; indeed, WT comparison between 6 and 24 months yielded reliable interaction between age and ISI [F (3,63) = 3; $p = 0.04$] due to much reduced PPF at 100 ms intervals ($t = 1,9$; $df = 21$, $p = 0.037$, t test one-tailed).

LTP

At all ages it was possible to induce a stable, long-lasting potentiation of synaptic transmission in hippocampal slices from WT mice. Analysis of the triple transgenic groups revealed significant, age-dependent deficits in LTP compared

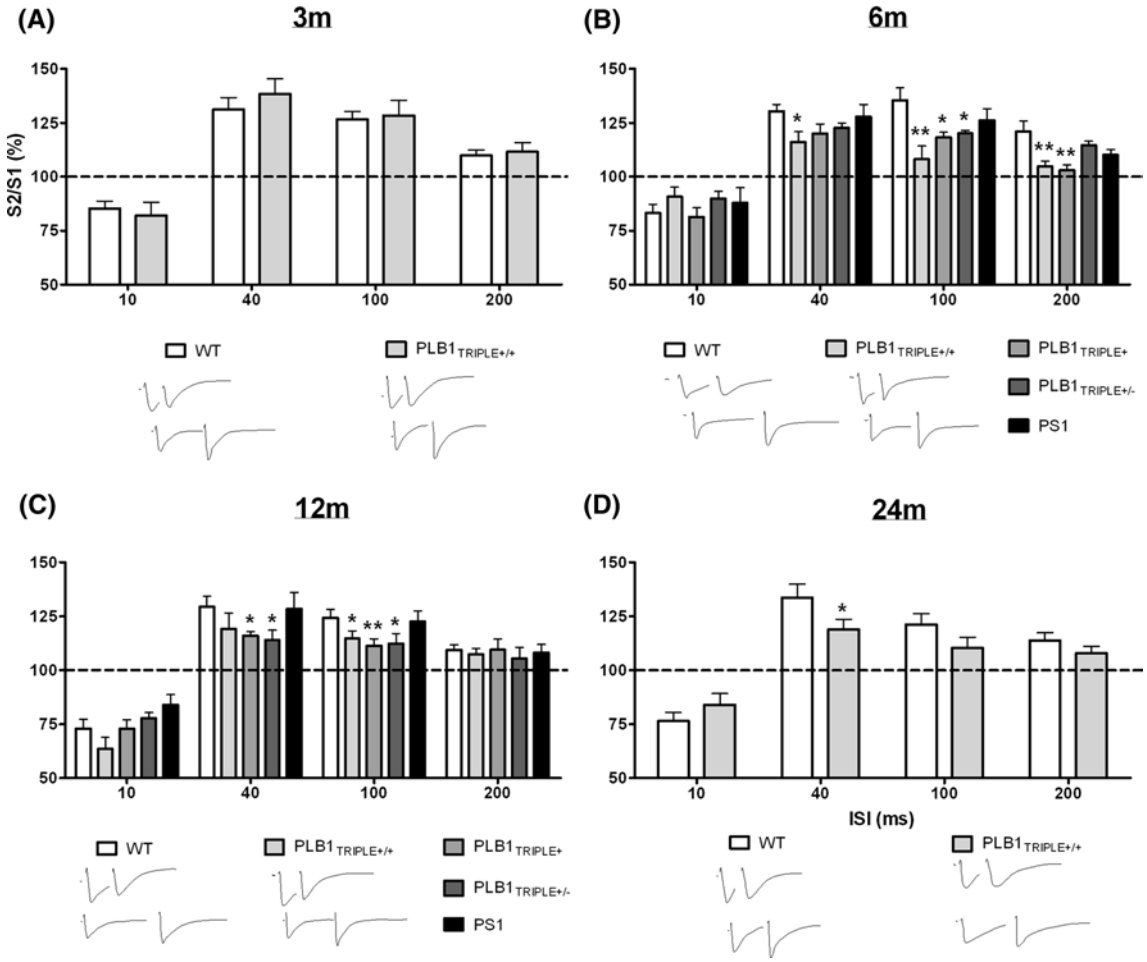

Fig. 7 Paired pulse facilitation is reduced in $PLB1_{Triple}$ mice from 6 months. **a** Paired pulse responses did not differ between $PLB1_{Triple+/+}$ ($n = 11$) and WT ($n = 16$) at 3 months. **b** Although intact in the PS1 group ($n = 10$), PPF was significantly reduced in the $PLB1_{Triple+/+}$ ($n = 10$), $PLB1_{Triple+}$ ($n = 11$), and $PLB1_{Triple+/-}$ ($n = 17$) groups versus WT ($n = 10$) at 6 months. **c** Similarly, $PLB1_{Triple+/+}$ ($n = 11$), $PLB1_{Triple+}$ ($n = 11$) and $PLB1_{Triple+/-}$ ($n = 11$) mice expressed deficits in PPF at 12 months compared with WT ($n = 16$), with no changes obvious in PS1 mice ($n = 10$). **d** PPF was also reduced in $PLB1_{Triple+/+}$ mice ($n = 12$) at 24 months relative to WT ($n = 14$). An overall ANOVA followed by individual *t* tests confirmed significant differences depicted for between selected data sets. Mean data for fEPSP slope 2/slope 1 ratios (S2/S1) + SEM are shown. $*p < 0.05$; $**p < 0.01$

with WT (Fig. 8). As seen for paired pulse responses, LTP was unaffected in 3 months old $PLB1_{Triple+/+}$ mice (Fig. 8a) and we did not examine any other genotypes.

At 6 months of age (Fig. 8b), there was a visible increase in fEPSP slopes post-tetanus in $PLB1_{Triple+/-}$ and WT groups, indicating stable STP, but it was not sustained and declined significantly to a value of 113 ± 4.1 % in $PLB1_{Triple+/-}$ 1 h post-tetanus compared with 136 ± 7.7 % in WT. This impression was confirmed statistically, producing an interaction between factors of genotype and time [F (59,2,124) = 1.4, $p < 0.05$]. Similar observations were made for $PLB1_{Triple+}$ and $PLB1_{Triple+/+}$ groups, albeit the statistical analyses revealed more robust effects [$PLB1_{Triple+}$: F (59,2,006) = 1.9, $p < 0.0001$; $PLB1_{Triple+/+}$: F (59,1,829) = 2.0, $p < 0.0001$]. Subsequent time point analysis (Student's *t* test) confirmed that responses from $PLB1_{Triple}$ were significantly different to WT at $t = 70$ (all p's < 0.0001) but not at $t = 11$. In the $PLB1_{Triple+}$ and $PLB1_{Triple+/+}$ groups, values at $t = 70$ min were not significantly different to baseline values indicating complete rundown of LTP.

At 12 months, similar findings emerged to those found at 6 months (Fig. 8c). Significant interactions in fEPSP slope relative to WT were evident in the $PLB1_{Triple+/-}$ [F (59,1,475) = 2.0, $p < 0.0001$], $PLB1_{Triple+}$ [F (59,1,534) = 3.7, $p < 0.0001$] and $PLB1_{Triple+/+}$ [F (59,1,770) = 2.8, $p < 0.0001$] groups. At $t = 70$ min, all triple transgenic groups differed reliably from WT (all p values < 0.0001).

LTP was also impaired in the $PLB1_{Triple+/+}$ group at 24 months of age (Fig. 8d) compared with WT [F (1,1,062) = 3.9, $p < 0.05$]. While the time course of the decline of LTP at 6 months was not significantly different to LTP at 12 months in any of the $PLB1_{Triple}$ groups, the

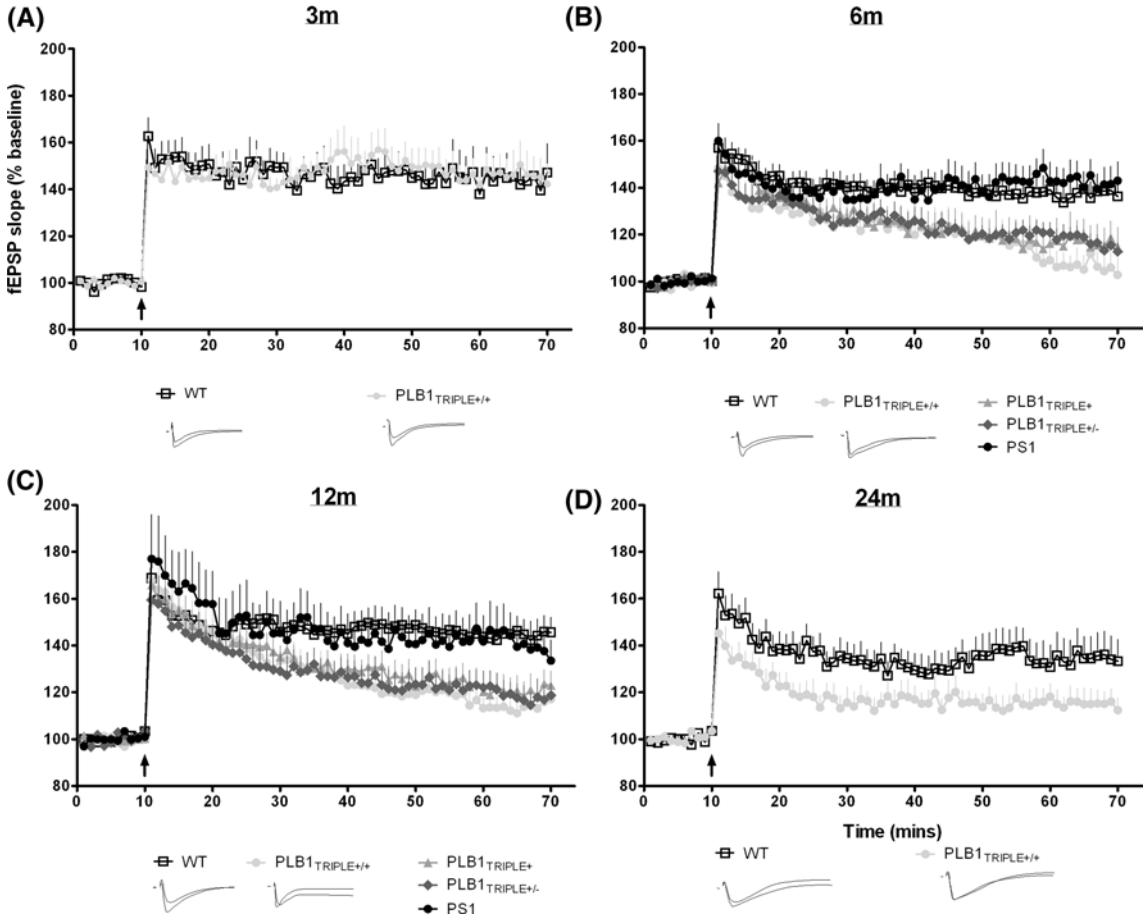

Fig. 8 Long-term potentiation is reduced in $PLB1_{Triple}$ mice from 6 months. **a** No changes in LTP were evident in $PLB1_{Triple+/+}$ ($n = 10$) mice at 3 months compared with WT ($n = 10$). **b** LTP was impaired in $PLB1_{Triple+/+}$ ($n = 11$), $PLB1_{Triple+}$ ($n = 13$), and $PLB1_{Triple+/-}$ ($n = 15$) groups versus WT ($n = 23$) at 6 months, and unaltered in PS1 mice ($n = 10$). For statistics, see text. **c** At 12 months, LTP was again intact in PS1 mice ($n = 10$) and reduced in $PLB1_{Triple+/+}$ ($n = 16$), $PLB1_{Triple+}$ ($n = 12$), and $PLB1_{Triple+/-}$ ($n = 11$) groups compared with WT ($n = 17$). **d** LTP was also impaired at 24 months in $PLB1_{Triple+/+}$ ($n = 10$) mice compared with WT ($n = 11$). Data of fEPSP slopes are shown as group means in % (+ SEM), relative to baseline; superimposed samples traces (baseline and 60 min post-tetanus) are also provided for selected groups

deficit observed in $PLB1_{Triple+/+}$ at 24 months was significantly different to that at 6 and 12 months (F values > 1.3; p values < 0.05) owing to a more rapid post-tetanus decline.

LTD

In a final series of experiments, we also assessed LTD in both WT and $PLB1_{Triple+/+}$ groups (Fig. 9). There was no deficit in $PLB1_{Triple+/+}$ mice at any age; robust and persistent depression was established following long-lasting slow-frequency stimulation and this was maintained during 1 h. Also, no age-related decay in LTD was obtained in brain slices from WT or $PLB1_{Triple+/+}$ mice.

Overall, the data presented here show deficits in basic synaptic transmission in aged $PLB1_{Triple}$ mice and deficits in short- and long-term plasticity from 6 months of age. Interestingly, the deficits in PPF and LTP did by and large not differ between $PLB1_{Triple+/-}$, $PLB1_{Triple+}$, and $PLB1_{Triple+/+}$ mice at 6 or 12 months even though the levels of gene expression and subsequent protein accumulation within cortical and hippocampal neurones in $PLB1_{Triple+/-}$ mice were approximately half of those in $PLB1_{Triple+/+}$ and $PLB1_{Triple+}$ mice. Moreover, the lack of differences between $PLB1_{Triple+/+}$ and $PLB1_{Triple+}$ mice indicates that gender has no bearing on the parameters investigated here.

Discussion

Previous studies in our laboratory have provided a first characterization of a novel knock-in triple transgenic mouse model of AD, $PLB1_{Triple}$ [14]. These mice presented with disease-relevant changes including tau and APP/Aβ pathology in the hippocampus, cognitive deficits in behavioral

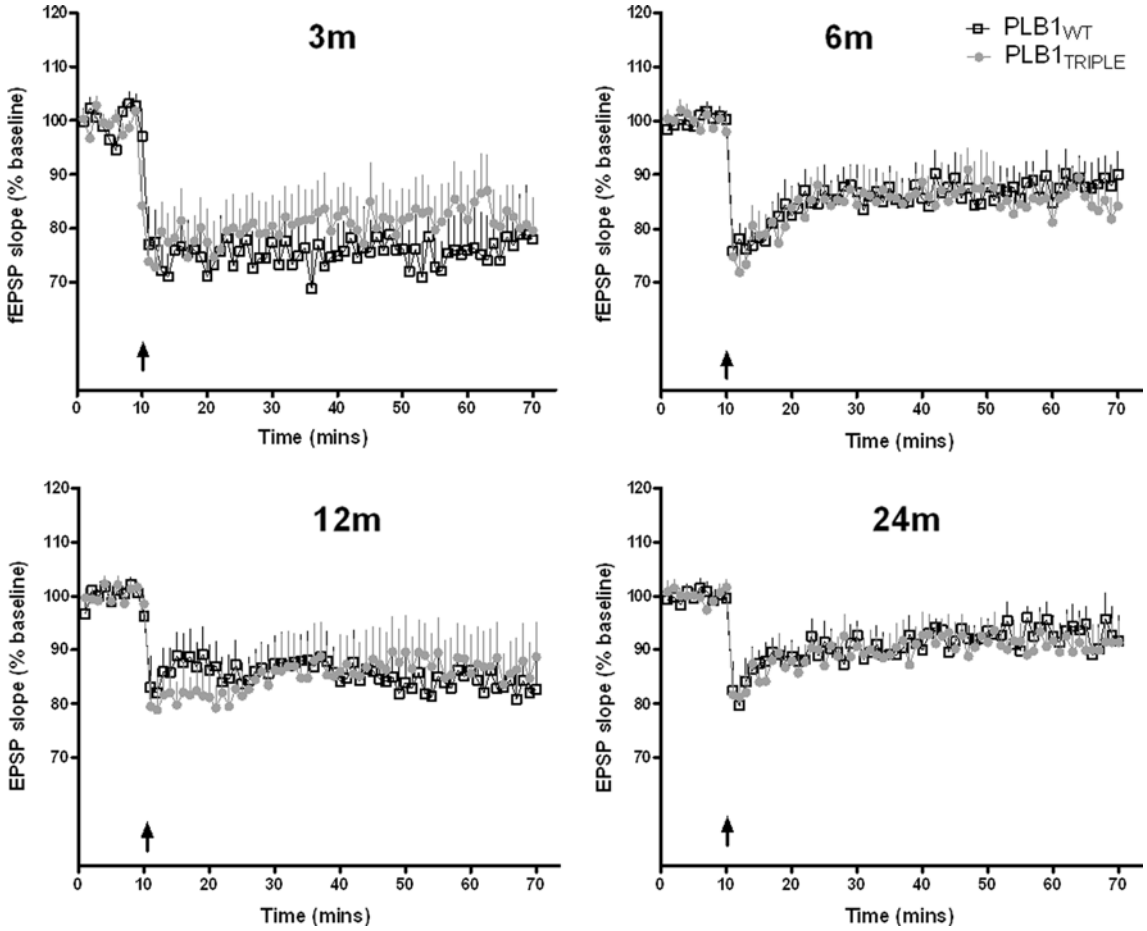

Fig. 9 Long-term depression is not altered in $PLB1_{Triple}$ mice. Hippocampal slices from four age groups [3 months (**a**), 6 months (**b**), 12 months (**c**), and 24 months (**d**)] of WT and $PLB1_{Triple+/+}$ mice revealed no genotype differences. LTD was readily induced by low-frequency stimulation of Schaffer collateral inputs to CA1 independent of age and genotype. All n's $\geq$ 8 for WT and n's $\geq$ 10 for $PLB1_{Triple+/+}$. Field EPSP slopes, calculated relative to baseline (in %), are shown (+ SEM)

paradigms (see also further behavioral data in [15]), alterations in sleep architecture, changes in brain glucose metabolism and deficits in hippocampal transmission and plasticity. The present study built upon these findings as we aimed to gain a richer understanding of the age-dependent changes in hippocampal physiology and plasticity, and its relationships with histopathological phenotypes. Towards this end, transcriptional tissue analysis, immunohistological identification of AD-like pathology, and investigation of hippocampal s ynaptic transmission and plasticity over a wide range of ages was undertaken in $PLB1_{Triple+/+}$, $PLB1_{Triple+}$, and $PLB1_{Triple+/-}$ mice. An overall summary of key results is provided in Table 1.

Perhaps the most comparable model to the $PLB1_{Triple}$ mice is the LaFerla 3xTg mouse, as it carries the same three risk genes (albeit with different mutations). Histological evidence and reported time for the onset of pathology in this mouse describe intracellular APP/Aβ accumulation from 6 months of age in a pre-plaque stage that preceded tau pathology, with robust tau accumulation and hyperphosphorylation (detected by AT-8) at <~15 months of age [6, 19]. In a later study, APP/Aβ pathology was already notable in the cortex and hippocampus as early as 2 months of age [20], tau accumulation was identified <6 months. The somewhat variable onset and progression of pathology may be caused by differences in inter-laboratory techniques or variation between gene expression in different breeding lines, typically problematic in pronuclear-derived models. However, the overall observation that amyloid preceded tau pathology was proposed as being consistent with the amyloid cascade hypothesis, but is in conflict with the earlier occurrence (and correlation with cognition) of tau pathology in humans, as well as the dissociation between plaque formation and cognitive abilities [21]. Further, the recent observation that tau pathology occurred in the absence of Aβ in the 3xTg mouse raises some questions regarding the link between these pathways [5], even more so since tau mutations alone are capable of inducing tau pathology [22]. Thus, the earlier

Table 1 Summary of electrophysiological and semi-quantitative immunohistochemical profiles in $PLB1_{Triple}$ mice

Genotype	IO curves	Paired pulse responses				LTP	LTD	Immunohistochemistry
		PPI	PPF					
			ISI = 40 ms	ISI = 100 ms	ISI = 200 ms			
Heterozygous ♀								
6 months	ns	ns	*	*	*	#	ns	–
12 months	ns	ns	*	**	***	### *	ns	Weak Aβ staining in cortex and hippocampus Diffuse staining of somata (pyramidal neurones); small plaques Less tau/Aβ immunoreactivity cf. homozygous
Hemizygous ♂								
6 months	ns	ns	ns	*	**	###	ns	NA
12 months	*	ns	*	**	ns	###	ns	NA
Homozygous ♀								
3 months	ns	ns	ns	ns	ns	ns	ns	Subtle somatic Aβ staining Tau expression in somata and neurites of cortex and hippocampus
6 months	ns	ns	*	*	ns	### *	ns	Rare and diffuse extracellular cortical and hippocampal plaques Increased tau expression in somata and neurites of cortex and hippocampus; P-tau identified in cortex and hippocampus
12 months	**	ns	*	**	ns	###	ns	Few diffuse extracellular cortical and hippocampal plaques increased intracellular Aβ staining (number and intensity) cf. 6 months age groups Increased tau expression in somata and neurites of cortex and hippocampus; increased P-tau identified in cortex and hippocampus
24 months	***	ns	*	ns	ns	*	ns	Few diffuse extracellular cortical and hippocampal plaques; intracellular Aβ staining extents into neuronal processes; increasing staining intensity with age[a] Decreased somatic tau expression cf. 12 months Increase of P-tau in somata, loss of P-tau from processes

IO input–output, *PPI* paired pulse inhibition, *PPF* paired pulse facilitation, *LTP* long-term potentiation, *LTD* long-term depression, *ISI* inter-stimulus interval, *P-tau* phospho-tau, *ns* not significant, *NA* not analyzed

* $p < 0.05$, ** $p < 0.01$, *** $p < 0.0001$ (genotype); ### $p < 0.0001$ (interaction) cf. wild-type

[a] Immunohistochemistry conducted in tissue from 21-month-old mice

emergence of amyloid-based pathologies in the 3xTg mouse may simply reflect differences in expression levels and/or limitations of the endogenous capability of mice to deal with amyloid vs. tau challenges. Here, tau expression in PLB_{Triple} mice preceded APP/amyloid detection and was apparent as early as 3 months of age, with a robust increase into adulthood. Hyperphosphorylated tau was also detected earlier (at 6 months) compared to 3xTg mice. The more prominent tau pathology may be due to the inclusion of multiple FTD mutations compared to the single mutation tau construct of the 3xTg mouse. A clear translocation of tau phosphorylation was also observed here with increasing age, moving from the processes into the somatic region of pyramidal neurons, thus mimicking a key early stage in tauopathy [23] and later-stage pathology of the 3xTg model (~12 months; [19]). The presence of AT-8 reactive phospho-tau (Ser-199, Ser-202, Thr-205) indicates abnormal tau phosphorylation, in keeping with reactivity towards these sites in PHF-tau extracted from human (diseased) samples [24, 25].

In comparison, the more diffuse APP/Aβ expression first observed at ~3 months in cortical tissue of $PLB1_{Triple}$ mice extended over time into hippocampal areas and into neuronal processes, with reliable intracellular APP/Aβ immunoreactivity detected from ~12 months of age. Maximal

amyloid pathology reached a stage comparable to that described in 12-month-old 3xTg as reported by Mastrangelo and Bowens [20], though few plaques were observed. Our previous quantification of aggregated amyloid in $PLB1_{Triple}$ mice confirmed significantly enhanced levels at 12 and 20 months in homozygous mice [14], a detailed analysis of age- and genotype-dependent changes of different amyloid and tau species will be subject to a follow-up publication.

Physiologically, we here uncovered significant deficits in basic synaptic transmission (IO relationships) in $PLB1_{Triple+/+}$ and $PLB1_{Triple+}$ mice older than 12 months of age; this parameter was intact at 6 months. Such an age-dependent progression corresponded with the increase in amyloid pathology and tau hyperphosphorylation as discussed above. Moreover, it appears that fiber volley amplitude as an index of pre-synaptic transmitter release is a more reliable indicator for synaptic impairments than stimulus-intensity based input–output relationships. Similar to the histological evidence, changes in synaptic transmission reported in other transgenic mouse models of AD vary somewhat, even for the same animal model. For example, synaptic transmission was found to be intact in Tg2567 mice in some studies, while significantly compromised in others (reviewed in [8]); this parameter seems overall more commonly affected in transgenic tau mice (e.g., [26, 27]). A corresponding impairment was also reported in the 3xTg mice at ~6 months [6], but this was not corroborated in follow-up reports [8]. From the present data, it is not possible to disentangle the roles of the APP and tau transgenes on the IO deficit witnessed; future studies in directly comparable single and double transgenic mice will be required for clarification. However, as tau was identified before changes in synaptic transmission were detectable, the presence of this protein alone may not be sufficient to significantly impair synaptic transmission. It thus appears likely that either amyloid alone, or in combination with tau/phospho-tau, is key for impaired synaptic transmission. Deficits in neural transmission have previously been linked to the overproduction of Aβ and resulting synapse loss, in addition to influences on calcium dynamics, mitochondrial function, and neurotransmitter release [28–30]. Other potentially contributing aspects, such as the specific role of soluble amyloid aggregates (ADDLs) and inflammatory responses, will be addressed in future investigations.

Both *short- (PPF) and long-term plasticity (LTP)* were also impaired in hippocampal slices from $PLB1_{Triple}$ mice. No changes in PPI were found, indicating that feedback inhibition is unaffected in our mice [31, 32]. PPF is a commonly assessed measure of short-term plasticity in transgenic models, caused by a residual presynaptic Ca^{2+} increase after the first stimulus, which results in enhanced neurotransmitter release [32, 33]. We found that PPF was impaired from 6 months of age in the $PLB1_{Triple}$ groups, confirming potential changes in presynaptic transmitter release in these mice. This is also in line with the observation that the most consistent changes were observed for shorter ISIs, nevertheless, an assessment of an additional interneuron involvement would require further analysis. Disruptions to PPF have been shown in some transgenic AD models previously (e.g., [33]), but the majority of studies have not reported such a phenotype [8]. Interestingly, an impairment of short-term plasticity [post-tetanic potentiation (PTP) in area CA3] has recently been proposed as potentially the earliest (at 2 months) anomaly in Tg2576 mice [28].

The molecular mechanisms underlying short-term plasticity are still largely unclear, although all are thought to be Ca^{2+}-dependent [34]. Fast synaptic plasticity such as PPF involves the binding of Ca^{2+} to an unknown facilitation sensor, which increases presynaptic Ca^{2+} currents by modifying Ca^{2+} entry through ion channels [35]. In cultured hippocampal neurones, APP has been demonstrated to influence Ca^{2+} processing by modifying ion fluxes and homeostasis. Crucially, the protein is transported within axons to the presynaptic terminal where it (or a fragment of it) is released upon processing, could potentially influence transmitter release [36–38]. Indeed, Aβ has been shown previously to impair PPF in the CA1 region of hippocampal slices, although some studies report conflicting data [39, 40]. It is also possible that tau, via its interaction with the microtubule network and resulting influence on vesicular dynamics, adversely affects PPF [41]. Our own data with viral transfection demonstrated that the expression of mutant APP, and more potently mutated tau, impairs axonal integrity and Ca^{2+} transients [42]. Here, PTP was unaltered in $PLB1_{Triple}$ mice at 6 and 12 months while PPF was reduced, suggesting that either the different stimulation protocols used to induce PTP and PPF rely on separate methods of expression. Alternatively, plasticity may result from similar presynaptic changes, but the stronger stimulation protocol used to induce PTP can overcome deficits revealed in PPF. The longer train of stimuli activates additional targets such as the endoplasmic reticulum and mitochondria, which may engage multiple effector mechanisms, including the modification of Ca^{2+} channels and activation of PKC [34, 43]. Deficits in these intracellular effector cascades may indeed be responsible for dissociations of PPF and PTP/LTP in CA1 of APP/PS1-21 mice [33], where PPF was normal in 8-month-old subjects while PTP (and LTP) was severely deficient, strongly suggesting that presynaptic release properties are less affected by amyloid accumulation.

In comparison to short-term plasticity, deficits in long-term plasticity and LTP in particular are common in transgenic AD mice incorporating mutations in APP, PS1, and/or tau [8]. Yet, even for this well-established protocol, contradictory data have been reported in the same model, e.g., both normal or impaired LTP in Tg2576 and 3xTg mice, which could either suggest variability of the animal model

or techniques employed, or indeed unsuitability of the paradigm as such. What is clear, however, is that heavy amyloid expression and plaque formation do not necessarily affect LTP; no such correlation could yet be established.

We here also uncovered deficits in LTP at 6 months and older. These deficits manifested as an impaired ability to maintain LTP, as PTP was intact in all groups, and did not worsen with age. Intriguingly, no deficits were observed in LTD supporting the notion that not all forms of plasticity are sensitive to transgenic disruption. Changes in synaptic plasticity correlated with the onset of Aβ pathology and phospho-tau detected at 6 months, but were preceded by intracellular tau labeling already apparent at 3 months. Although it is not possible to assign the changes witnessed to either protein, comparable deficits occurred in all $PLB1_{Triple}$ genotypes even though gene expression was reduced approximately twofold and immunoreactivity was very weak in $PLB1_{Triple+/-}$ mice. Our data therefore suggest that there is no direct correlation between the degree of total amyloid and/or tau expression and the extend of LTP impairments.

Few experimental studies exist on LTD in transgenic AD models, these have revealed no deficits in Tg2576 mice at fronto-striatal synapses [44, 45], and enhanced CA1 LTD amidst normal LTP at 3 months [45]. Yet, CA1 LTD was suppressed in old (>15 months) APP/PS1-bearing mice [46], suggesting a more severe phenotype in aged bigenic animals. At the same time, however, these data contradict studies with pharmacologically applied Aβ protein dimers isolated from AD brains, which facilitated LTD but inhibited LTP [2]. Importantly, a recent LTD study in 2-month-old 3xTg mice suggests that seemingly unaltered LTD may still be based on differing and compensatory cellular mechanisms [47], an observation that requires further research in our model.

There were no gender-related differences observed in $PLB1_{Triple}$ mice; hemizygous males and homozygous females were comparable in all electrophysiological parameters. This is not entirely surprising due to the knock-in procedure used in their generation resulting in the expression of one transgene only, and X-inactivation ensuring that only one copy of the transgene was transcribed in female mice. Indeed, comparable levels of mRNA were transcribed from the APP and tau genes in hemizygous and homozygous groups. Sexual dimorphism has been reported previously in AD models, particularly in 3xTg-AD mice [6, 48, 49] but appears not to be relevant here. In AD patients, a gender bias is reported for females over the age of 80 years [50], but gender-related life style factors not applicable to animal studies may be responsible [51].

In conclusion, $PLB1_{Triple}$ mice developed age-dependent and progressive physiological deficits in the presence of low levels of protein build-up. This indicates that aggressive protein accumulation is not essential when modeling AD in transgenic mice, and other biomarkers may provide more reliable endophenotypes. The data presented here, combined with those from previous studies [14, 16], further highlight the potential of $PLB1_{Triple}$ mice as a highly relevant transgenic model of AD and call for the examination of single and double transgenic mice to dissect the roles of individual genes in the physiological phenotypes revealed here.

References

1. LaFerla FM, Oddo S (2005) Alzheimer's disease: Abeta, tau and synaptic dysfunction. Trends Mol Med 11:170–176
2. Shankar GM, Walsh DM (2009) Alzheimer's disease: synaptic dysfunction and Abeta. Mol Neurodegener 4:48
3. Brouillette J, Caillierez R, Zommer N, Alves-Pires C, Benilova I, Blum D, De Strooper B, Buee L (2012) Neurotoxicity and memory deficits induced by soluble low-molecular-weight amyloid-beta1-42 oligomers are revealed in vivo by using a novel animal model. J Neurosci 32:7852–7861
4. Platt B (2006) Experimental approaches to assess metallotoxicity and ageing in models of Alzheimer's disease. J Alzheimers Dis 10:203–213
5. Winton MJ, Lee EB, Sun E, Wong MM, Leight S, Zhang B, Trojanowski JQ, Lee VM (2011) Intraneuronal APP, not free Abeta peptides in 3xTg-AD mice: implications for tau versus Abeta-mediated Alzheimer neurodegeneration. J Neurosci 31:7691–7699
6. Oddo S, Caccamo A, Shepherd JD, Murphy MP, Golde TE, Kayed R, Metherate R, Mattson MP, Akbari Y, LaFerla FM (2003) Triple-transgenic model of Alzheimer's disease with plaques and tangles: intracellular Abeta and synaptic dysfunction. Neuron 39:409–421
7. Smith IF, Green KN, LaFerla FM (2005) Calcium dysregulation in Alzheimer's disease: recent advances gained from genetically modified animals. Cell Calcium 38:427–437
8. Marchetti C, Marie H (2011) Hippocampal synaptic plasticity in Alzheimer's disease: what have we learned so far from transgenic models? Rev Neurosci 22:373–402
9. Platt B, Carpenter DO, Busselberg D, Reymann KG, Riedel G (1995) Aluminum impairs hippocampal long-term potentiation in rats in vitro and in vivo. Exp Neurol 134:73–86
10. Hall AM, Roberson ED (2012) Mouse models of Alzheimer's disease. 88:3–12
11. Gama Sosa MA, De Gasperi R, Elder GA (2010) Animal transgenesis: an overview. Brain Struct Funct 214:91–109
12. Deng HX, Siddique T (2000) Transgenic mouse models and human neurodegenerative disorders. Arch Neurol 57:1695–1702
13. Schenk D, Hagen M, Seubert P (2004) Current progress in beta-amyloid immunotherapy. Curr Opin Immunol 16:599–606
14. Platt B, Drever B, Koss D, Stoppelkamp S, Jyoti A, Plano A, Utan A, Merrick G, Ryan D, Melis V, Wan H, Mingarelli M, Porcu E, Scrocchi L, Welch A, Riedel G (2011) Abnormal cognition, sleep, EEG and brain metabolism in a novel knock-in Alzheimer mouse, PLB1. PLoS ONE 6:e27068
15. Ryan D, Koss D, Porcu E, Robinson L, Platt B and Riedel G (CMLS, submitted) Spatial learning impairments in $PLB1_{Triple}$ knock-in Alzheimer mice are task-specific and age-dependent
16. Platt B, Welch A, Riedel G (2011) FDG-PET imaging, EEG and sleep phenotypes as translational biomarkers for research in Alzheimer's disease. Biochem Soc Trans 39:874–880
17. Jyoti A, Plano A, Riedel G, Platt B (2010) EEG, activity, and sleep architecture in a transgenic AbetaPPswe/PSEN1A246E Alzheimer's disease mouse. J Alzheimers Dis 22:873–887

18. Drever BD, Anderson WG, Johnson H, O'Callaghan M, Seo S, Choi DY, Riedel G, Platt B (2007) Memantine acts as a cholinergic stimulant in the mouse hippocampus. J Alzheimers Dis 12:319–333
19. Oddo S, Caccamo A, Kitazawa M, Tseng BP, LaFerla FM (2003) Amyloid deposition precedes tangle formation in a triple transgenic model of Alzheimer's disease. Neurobiol Aging 24:1063–1070
20. Mastrangelo MA, Bowers WJ (2008) Detailed immunohistochemical characterization of temporal and spatial progression of Alzheimer's disease-related pathologies in male triple-transgenic mice. BMC Neurosci 9:81
21. Nelson PT et al (2012) Correlation of Alzheimer disease neuropathologic changes with cognitive status: a review of the literature. J Neuropathol Exp Neurol 71:362–381
22. Gotz J, Gladbach A, Pennanen L, van Eersel J, Schild A, David D, Ittner LM (2010) Animal models reveal role for tau phosphorylation in human disease. Biochim Biophys Acta 1802:860–871
23. Braak E, Braak H (1997) Alzheimer's disease: transiently developing dendritic changes in pyramidal cells of sector CA1 of the Ammon's horn. Acta Neuropathol 93:323–325
24. Morishima-Kawashima M, Hasegawa M, Takio K, Suzuki M, Yoshida H, Watanabe A, Titani K, Ihara Y (1995) Hyperphosphorylation of tau in PHF. Neurobiol Aging 16:365–380
25. Wang JZ, Grundke-Iqbal I, Iqbal K (2007) Kinases and phosphatases and tau sites involved in Alzheimer neurofibrillary degeneration. Eur J Neurosci 25:59–68
26. Tanemura K, Murayama M, Akagi T, Hashikawa T, Tominaga T, Ichikawa M, Yamaguchi H, Takashima A (2002) Neurodegeneration with tau accumulation in a transgenic mouse expressing V337 M human tau. J Neurosci 22:133–141
27. Yoshiyama Y, Kojima A, Ishikawa C, Arai K (2010) Anti-inflammatory action of donepezil ameliorates tau pathology, synaptic loss, and neurodegeneration in a tauopathy mouse model. J Alzheimers Dis 22:295–306
28. Lee SH, Kim KR, Ryu SY, Son S, Hong HS, Mook-Jung I, Lee SH, Ho WK (2012) Impaired short-term plasticity in mossy fiber synapses caused by mitochondrial dysfunction of dentate granule cells is the earliest synaptic deficit in a mouse model of Alzheimer's disease. J Neurosci 32:5953–5963
29. Demuro A, Parker I, Stutzmann GE (2010) Calcium signaling and amyloid toxicity in Alzheimer disease. J Biol Chem 285:12463–12468
30. Shankar GM, Bloodgood BL, Townsend M, Walsh DM, Selkoe DJ, Sabatini BL (2007) Natural oligomers of the Alzheimer amyloid-beta protein induce reversible synapse loss by modulating an NMDA-type glutamate receptor-dependent signaling pathway. J Neurosci 27:2866–2875
31. Leung LS, Peloquin P, Canning KJ (2008) Paired-pulse depression of excitatory postsynaptic current sinks in hippocampal CA1 in vivo. Hippocampus 18:1008–1020
32. Platt B, Withington DJ (1997) Paired-pulse depression in the superficial layers of the guinea-pig superior colliculus. Brain Res 777:131–139
33. Gengler S, Hamilton A, Holscher C (2010) Synaptic plasticity in the hippocampus of a APP/PS1 mouse model of Alzheimer's disease is impaired in old but not young mice. PLoS ONE 5:e9764
34. Zucker RS, Regehr WG (2002) Short-term synaptic plasticity. Annu Rev Physiol 64:355–405
35. Catterall WA, Few AP (2008) Calcium channel regulation and presynaptic plasticity. Neuron 59:882–901
36. Koo EH, Sisodia SS, Archer DR, Martin LJ, Weidemann A, Beyreuther K, Fischer P, Masters CL, Price DL (1990) Precursor of amyloid protein in Alzheimer disease undergoes fast anterograde axonal transport. Proc Natl Acad Sci USA 87:1561–1565
37. Schubert W, Prior R, Weidemann A, Dircksen H, Multhaup G, Masters CL, Beyreuther K (1991) Localization of Alzheimer beta A4 amyloid precursor protein at central and peripheral synaptic sites. Brain Res 563:184–194
38. Koizumi S, Ishiguro M, Ohsawa I, Morimoto T, Takamura C, Inoue K, Kohsaka S (1998) The effect of a secreted form of beta-amyloid-precursor protein on intracellular Ca2 + increase in rat cultured hippocampal neurones. Br J Pharmacol 123:1483–1489
39. Freir DB, Holscher C, Herron CE (2001) Blockade of long-term potentiation by beta-amyloid peptides in the CA1 region of the rat hippocampus in vivo. J Neurophysiol 85:708–713
40. Schmid AW, Freir DB, Herron CE (2008) Inhibition of LTP in vivo by beta-amyloid peptide in different conformational states. Brain Res 1197:135–142
41. Zhang B, Maiti A, Shively S, Lakhani F, McDonald-Jones G, Bruce J, Lee EB, Xie SX, Joyce S, Li C, Toleikis PM, Lee VM, Trojanowski JQ (2005) Microtubule-binding drugs offset tau sequestration by stabilizing microtubules and reversing fast axonal transport deficits in a tauopathy model. Proc Natl Acad Sci USA 102:227–231
42. Stoppelkamp S, Bell HS, Palacios-Filardo J, Shewan DA, Riedel G, Platt B (2011) In vitro modelling of Alzheimer's disease: degeneration and cell death induced by viral delivery of amyloid and tau. Exp Neurol 229:226–237
43. Tang Y, Zucker RS (1997) Mitochondrial involvement in post-tetanic potentiation of synaptic transmission. Neuron 18:483–491
44. Middei S, Geracitano R, Caprioli A, Mercuri N, Ammassari-Teule M (2004) Preserved fronto-striatal plasticity and enhanced procedural learning in a transgenic mouse model of Alzheimer's disease overexpressing mutant hAPPswe. Learn Mem 11:447–452
45. D'Amelio M, Cavallucci V, Middei S, Marchetti C, Pacioni S, Ferri A, Diamantini A, De Zio D, Carrara P, Battistini L, Moreno S, Bacci A, Ammassari-Teule M, Marie H, Cecconi F (2011) Caspase-3 triggers early synaptic dysfunction in a mouse model of Alzheimer's disease. Nat Neurosci 14:69–76
46. Chang EH, Savage MJ, Flood DG, Thomas JM, Levy RB, Mahadomrongkul V, Shirao T, Aoki C, Huerta PT (2006) AMPA receptor downscaling at the onset of Alzheimer's disease pathology in double knockin mice. Proc Natl Acad Sci USA 103:3410–3415
47. Chakroborty S, Kim J, Schneider C, Jacobson C, Molgo J, Stutzmann GE (2012) Early presynaptic and postsynaptic calcium signaling abnormalities mask underlying synaptic depression in presymptomatic Alzheimer's disease mice. J Neurosci 32:8341–8353
48. Lewis J, Dickson DW, Lin WL, Chisholm L, Corral A, Jones G, Yen SH, Sahara N, Skipper L, Yager D, Eckman C, Hardy J, Hutton M, McGowan E (2001) Enhanced neurofibrillary degeneration in transgenic mice expressing mutant tau and APP. Science 293:1487–1491
49. Clinton LK, Billings LM, Green KN, Caccamo A, Ngo J, Oddo S, McGaugh JL, LaFerla FM (2007) Age-dependent sexual dimorphism in cognition and stress response in the 3xTg-AD mice. Neurobiol Dis 28:76–82
50. Vina J, Lloret A (2010) Why women have more Alzheimer's disease than men: gender and mitochondrial toxicity of amyloid-beta peptide. J Alzheimers Dis 20(Suppl 2):S527–S533
51. Arab L, Sabbagh MN (2010) Are certain lifestyle habits associated with lower Alzheimer's disease risk? J Alzheimers Dis 20:785–794